

Real and virtual photon structure from dijet events

J. Cvach ^{a*}

^aInstitute of Physics, Academy of Sciences of the Czech Republic,
Na Slovance 2, 182 21 Praha, Czech Republic

Talk given on behalf of the H1 Collaboration at the 7th International Workshop on Deep Inelastic Scattering and QCD DIS99, Zeuthen, April 19–23, 1999.

Jet production in ep collisions is sensitive to the partonic structure of photon. The latest measurements of dijet production from the H1 experiment provide new results of the gluon density of real photons at low x and, for the first time, on the partonic density of virtual photons. Properties of the photon remnant were measured as a function of the hard scale defined by the p_T of the jets. The comparison of dijet cross sections with the NLO QCD calculation shows the non-triviality of the concept of virtual photon structure.

1. INTRODUCTION

The experiments carried out in the last 15 years at PETRA, PEP, TRISTAN and recently also at LEP and HERA have shown convincingly that due to strong interactions the real photon has a nontrivial hadron-like structure. In these experiments incoming electrons or positrons acted as a source of virtual photons which were subsequently involved in hard collisions with partons from another photon or proton. Most of these studies concerned the region of very small photon virtualities Q^2 (typically $\leq 1 \text{ GeV}^2$ — called photoproduction). With increasing Q^2 the situation changes as photon has less time to develop its hadronic structure. The way the photon structure varies with Q^2 holds important information on the interplay between perturbative and non-perturbative aspects of QCD.

Contrary to e^+e^- colliders which are sensitive via deep inelastic $\gamma^*\gamma$ scattering to the quark structure of the real photon, jet production at the ep collider HERA is sensitive both to gluon and quark structure of photon. Moreover the jet cross section at HERA is large enough to allow us to investigate the structure not only of real $Q^2 < 10^{-2} \text{ GeV}^2$ but also of virtual photon ($1.6 \leq Q^2 \leq 80 \text{ GeV}^2$ in this paper). All results reported here were obtained in e^+p collisions at

energies $(27.6 + 820) \text{ GeV}$.

2. GLUON DENSITY OF REAL γ

The dijet cross section in ep collisions at HERA is sensitive to the gluon content of photon especially at lower x_γ .² To reach x_γ as low as 0.04 the inelasticity of the reaction was restricted to $0.5 < y < 0.7$ in photoproduction data of integrated luminosity $\sim 7.2 \text{ pb}^{-1}$. Jets were obtained by the CDF cone algorithm with $R = 0.7$ and accepted in the pseudorapidity range $-0.2 < \eta_i < 2.5$ in laboratory frame.³ The cross section $d\sigma/dx_\gamma$ from events with at least two jets with $E_{T,i} > 6 \text{ GeV}$ after pedestal subtraction and $|\eta_1 - \eta_2| < 1$ was corrected for detector inefficiencies using PHOJET and PYTHIA.

To obtain the gluon density of the photon the dijet cross section was further unfolded to parton level using D'Agostini's program [1]. The largest systematic error in the resulting effective parton density

$$f_\gamma(x_\gamma, Q^2, E_T^2) = \sum_i^{N_f} (q_i + \bar{q}_i) + \frac{9}{4}g. \quad (1)$$

where q_i, \bar{q}_i, g are the quark, antiquark and gluon densities in the photon, comes from the hadronic

² x_γ is the fraction of photon momentum carried by parton.

³The $+z$ axis of the coordinate system points in the direction of incoming proton.

*Supported by GA AV ČR grant no. A1010821.

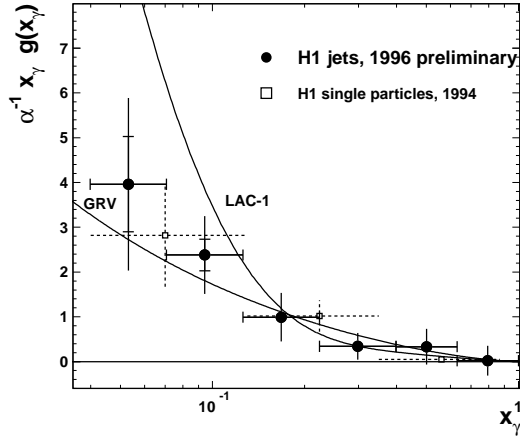


Figure 1. Measurement of gluon density in real photon from dijet (\bullet - this analysis) and high p_T track (\square) events.

E scale uncertainty and different treatment of soft parton interactions used in PHOJET and PYTHIA. The both dominate at low x_γ . The measured effective parton density is almost independent of the hard scale defined by the p_T of the partons. The gluon density is obtained from the effective parton density subtracting quark densities as given by the GRV-LO parametrisation.

The result of [2] is shown in Fig 1 together with the H1 analysis of high p_T inclusive tracks [3]. Both measurements are consistent with the increase of gluon density in real photon at low x_γ . Note that the high p_T inclusive track and the jet analyses are subject to different detector systematics. The growth of $g(x_\gamma)$ at low x_γ agrees with the GRV-LO parametrisation.

3. PARTON DENSITY OF VIRTUAL γ^*

The purpose of this analysis is to investigate the evolution of the effective parton density (1) with Q^2 and with the hard scale P_t . Jets were found using the inclusive k_T algorithm. Events were accepted if the two highest E_T jets in the

event were in the backward hemisphere of the γ^*p cms frame with $|\eta_1 - \eta_2| < 1$, $-3 < \bar{\eta} < -0.5$, where η_i are jet rapidities and $\bar{\eta}$ their average. The constraints on jet E_T were such that no jet has $E_T < 4$ GeV and the sum of jet E_T 's is always ≥ 11 GeV. The inelasticity of reaction was restricted to $0.1 < y < 0.7$ and virtuality of γ^* to $1.6 < Q^2 < 80$ GeV². The integrated luminosity of the data sample is ~ 6 pb⁻¹. The triple-differential jet cross section $d\sigma/dQ^2 d\bar{E}_T^2 dx_\gamma$ was measured [4], where \bar{E}_T is the mean transverse energy of the two highest E_T jets. From the cross section a leading order effective parton density as a function of x_γ , Q^2 , P_t^2 was extracted. For unfolding [1] the correlation matrix was used based on HERWIG and RAPGAP Monte Carlo samples. The largest systematic error $\sim 25\%$ in the parton density arises from model dependence (hadronization uncertainty).

The effective parton density was extracted in the kinematic range of $0.15 < x_\gamma < 0.75$ and $30 < \bar{E}_T^2 < 300$ GeV² in bins of Q^2 , P_t^2 and x_γ with limitation $\langle P_t^2 \rangle > \langle Q^2 \rangle$. The parton density is approximately independent of P_t^2 , and within errors, it is consistent with the normalisation and logarithmic scaling violations characteristic of the photon structure. The logarithmic suppression with increasing Q^2 as predicted by virtual photon structure gives a good description below $Q^2 \sim 20$ GeV² (Fig 2). Comparison with a ρ pole model shows that the nonperturbative VDM component plays significant role only in the parton density of the real photon.

4. PHOTON REMNANT

When only a fraction of the photon momentum is involved in the hard collision then the remaining momentum is carried away by spectator partons. These partons fragment into a photon remnant which is expected to be approximately collinear with the original photon. There are at least two possible ways to study the properties of the photon remnant. One is to treat it as an energy deposit close to the direction of the photon, the other to find it as a low p_T jet by jet algorithms. In the analysis [6] the $\langle p_t \rangle$ of photon remnant was measured as a function of the photon

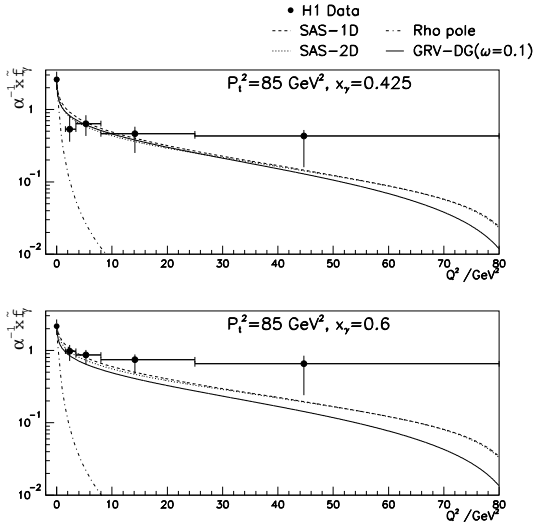


Figure 2. The leading order effective parton density of the photon as a function of Q^2 at $P_t^2 = 85 \text{ GeV}^2$. The errors are dominated by systematics. Shown are also GRV and SAS photon parton densities and photoproduction data scaled by a ρ pole factor (dot-dashed curve).

virtuality $Q^2 < 25 \text{ GeV}^2$ and $(p_{T,1} + p_{T,2}) > 12 \text{ GeV}$ of two jets using the DECO [5] jet algorithm. Jets are accepted in pseudorapidity range of $-3 < \eta < 0$ in γ^*p cms and $x_\gamma < 0.75$.

The $d\sigma/dp_t$ distribution [6] of the photon remnant corrected for detector effects agrees better with HERWIG than RAPGAP models. The intrinsic momentum k_t of the parton coming to the hard process is taken as Gaussian with $k_0 = 0.66 \text{ GeV}$ to describe relatively high $\langle p_t \rangle \sim 2 \text{ GeV}$ observed in data. It was found that hadronization effects contribute $\sim 1 \text{ GeV}$ to this value but do not change the $d\sigma/dp_t$ dependence. Fig 3 shows the dependence of average p_t of the photon remnant on the hard scale given by p_T of jets. Comparison of photoproduction ($Q^2 < 0.01$) and low Q^2 ($1.4 < Q^2 < 25 \text{ GeV}^2$) data shows no significant dependence on the photon virtuality. On

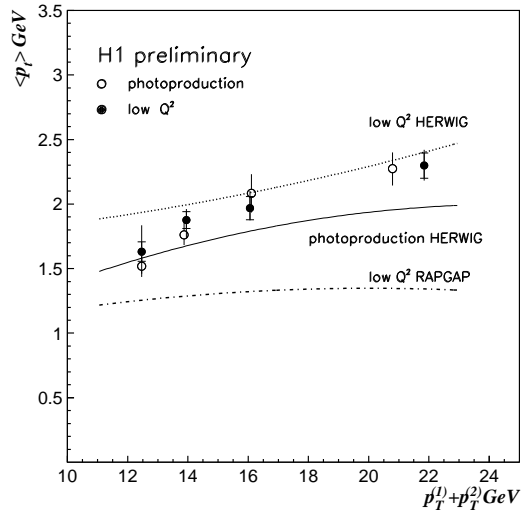


Figure 3. Average $\langle p_t \rangle$ of photon remnant for photoproduction (\circ) and low Q^2 (\bullet) data as a function of $p_{T,1} + p_{T,2}$ of two jets.

the other hand $\langle p_t \rangle$ of the photon remnant is correlated with the hard scale of the process — it increases with p_T of jets.

5. COMPARISON WITH NLO

For the virtual photon with $Q^2 \geq 1 \text{ GeV}^2$ the concept of photon structure is in principal not needed since a part of its effects is included in NLO diagrams. Therefore the question arises whether in NLO the photon structure function is still needed for the description of data. To answer this question the dijet cross section was compared with NLO calculation of JETVIP [7].

Jets were obtained by the CDF cone algorithm applied to data of integral luminosity of $\sim 1 \text{ pb}^{-1}$ in the range $1.4 < Q^2 < 25 \text{ GeV}^2$. Two jets with the highest E_T had to fulfil conditions $E_{T,1} > 7, E_{T,2} > 5 \text{ GeV}$ in the pseudorapidity range $-3 < \eta_{1,2} < 0$ in the γ^*p cms.

The $d\sigma/d\eta$ distribution of inclusive dijet production in four Q^2 bins is given in Fig 4 [8].

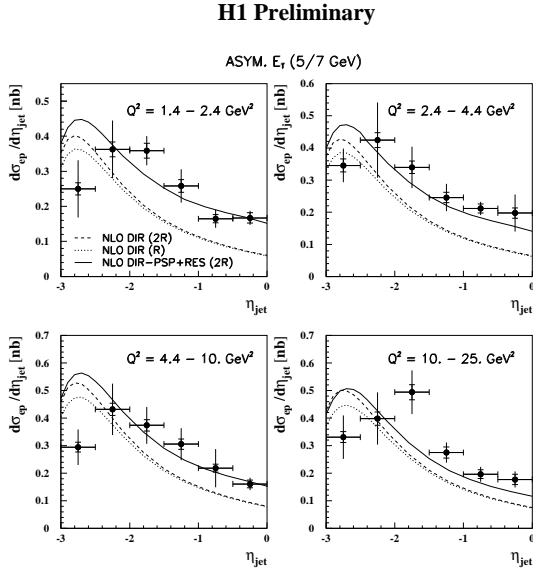


Figure 4. The dijet inclusive cross section as a function of jet pseudorapidity η . Data points (\bullet) are compared to NLO calculation of program JETVIP.

The data are corrected for detector inefficiencies. The curves represent NLO calculation by JETVIP. The dashed line represents the contribution from unsubtracted NLO direct processes (no structure function of the virtual photon — for details see [9]). The full line corresponds to the full NLO calculation including also diagrams from resolved processes with GRV-HO parton distribution functions. We see that for $\eta > -2.5$ and $Q^2 < 10 \text{ GeV}^2$ the unsubtracted direct NLO calculation is systematically below the data. On the other hand, the full NLO calculation (solid curve) is in a reasonable agreement with data in all four Q^2 bins.

Since hadronization corrections are not included in the NLO parton level calculation, deviations from the measured cross section are expected. Estimates show that they increase significantly at $\eta < -2.5$ being at the level of $\sim 10\%$

at larger pseudorapidity.

Acknowledgements: Thanks to all those who contributed to the analyses presented here. I want to thank to J. Chýla for helpful discussions. The financial support from the DIS99 Organising Committee is gratefully acknowledged.

REFERENCES

1. G. D'Agostini, Nucl. Instr. and Meth. A362 (1995) 487.
2. O. Kaufmann, Workshop on new results from HERA, Ringberg Castle 1999 and PhD Thesis, Heidelberg 1998, unpublished.
3. H1 Collaboration, C. Adloff et al., DESY 98-148 (1998).
4. H1 Collaboration, C. Adloff et al., DESY 98-205 (1998).
5. G. Knies, A. Valkárová, DESY 94-047 (1994).
6. A. Valkárová, Proceedings of PHOTON 99, Freiburg im Breisgau.
7. B. Pötter, Comp. Phys. Comm. 119 (1999) 45.
8. M. Taševský, PhD Thesis, Praha 1999, in preparation.
9. G. Kramer, B. Pötter, Eur. Phys. J. C5 (1998) 665.